

# Micromanipulation, communication and swarm intelligence issues in a swarm microrobotic platform

P. Valdastrì<sup>a,\*</sup>, P. Corradi<sup>a</sup>, A. Menciassi<sup>a</sup>, T. Schmickl<sup>b</sup>, K. Crailsheim<sup>b</sup>, J. Seyfried<sup>c</sup>, P. Dario<sup>a</sup>

<sup>a</sup> *Scuola Superiore Sant'Anna - CRIM Lab, V.le R. Piaggio 34 – 56025 Pontedera (PI), Italy*

<sup>b</sup> *Department for Zoology, Karl-Franzens-Universität Graz, Universitätsplatz 2, A-8010 Graz, Austria*

<sup>c</sup> *Universität Karlsruhe (TH), IPR, Building 40.28, Kaiserstraße 12 – 76128 Karlsruhe, Germany*

Received 18 April 2005; received in revised form 8 May 2006; accepted 15 May 2006

Available online 5 July 2006

## Abstract

Rapid advancements of both microsystem technology and multi-agent systems have generated a new discipline, arising from the fusion of microrobotics technologies and of swarm intelligence theories. Microrobotics contributes with new capabilities in manipulating objects in the microscale and in developing miniaturized intelligent machines, while swarm intelligence supplies new algorithms allowing sets of simple robotic agents to solve complex tasks. A microrobotic swarm that is able to collectively achieve a cleaning task in an arena has been developed. This paper presents a novel platform for microrobotic swarms with the goal to apply swarm intelligence results to practical micromanipulation tasks and describes in details two main features of the platform: an optical communication strategy between the microrobotic agents, in order to share information and to coordinate swarm actions, and a micromanipulation technique – based on electrostatic phenomena – which can be performed by each microrobotic agent.

© 2006 Elsevier B.V. All rights reserved.

**Keywords:** Microrobotics; Swarm intelligence; Optical communication; Electrostatic grasping; Electrostatic releasing

## 1. Microrobotics and swarm robotics

A growing worldwide interest in microrobotic devices is today evident, including micromanipulation tools and microconveyers and/or microrobots as locomotive mechanisms. The general term “microrobots” can be better classified into three different subcategories:

- Miniature robots or minirobots: size on the order of a few cubic centimeters and fabricated by assembling conventional miniature components;
- MEMS-based microrobots (or microrobots): a sort of “modified chip” fabricated by silicon MEMS-based technologies having features in the micrometer range;
- Nanorobots: scale similar to the biological cell (on the order of a few hundred nanometers) and fabricated by molecular engineering.

Microrobotics has a particular relevance in the development of a relatively new scientific discipline named “Swarm Robotics”. Swarm robotics can be defined as the study of how a large number of relatively simple agents can be constructed/programmed to collectively accomplish tasks that are beyond the capabilities of a single one. Differently from other studies on multi-agent systems, swarm robotics focuses on the concepts of self-organization and emergent behaviors, while considering the issues of scalability and robustness. This aspect involves the use of relatively simple robots with local sensing abilities, and the exploitation of scalable communication mechanisms and decentralized control strategies. It is in the perspective of miniaturization that swarm-based robotics becomes meaningful [7], therefore leading to the concept of “swarm microrobotics”. “Microrobotic Swarms” consist of hundreds of mobile robots, a few cubic millimeters in size. The capabilities of the single unit are consequently limited and, therefore, microrobots need to operate in very large groups or swarms to affect the macroworld. Mass fabrication microtechnologies have the potential to produce a large number

\* Corresponding author. Fax: +39 050883497.  
E-mail address: [pietro@sssup.it](mailto:pietro@sssup.it) (P. Valdastrì).

of units at low costs, while the swarm intelligence approach can compensate the limited capabilities of the single units – due to their size – with an emergent coordinated and collaborative swarm behavior. Currently, there are several ongoing projects that aim to develop and control large numbers of physically embodied agents. Self-organizing and cooperative behaviours have been investigated for navigation, for pattern formation [34,38,55], and for doing tasks too complex or impossible for a single robot to achieve [8], like cooperative pushing [27]. Decentralized control and reactive behaviour on local perception have been implemented for object clustering tasks [5,20,30] and object sorting [32].

A very promising branch of swarm robotics is self-assembly swarm-based robotics. This discipline studies systems in which quite small and capability-limited robotic modules can assemble and reconfigure autonomously in larger robotic structure capable of performing tasks that the single sub-module is not able to. The concept was first investigated in [39] and introduced in robotics in [19]. Main realizations are addressed in [13,22,35,37].

## 2. The I-SWARM project: Objectives and addressed issues

The I-SWARM project (Intelligent-Small World Autonomous Robots for Micromanipulation, <http://www.i-swarm.org>) combines expertise and knowledge in microrobotics, in distributed and adaptive systems as well as in self-organizing biological swarms. By exploiting advanced fabrication technologies, the project goal is to mass-produce many microrobots which can then be employed as a “real” swarm consisting of up to 1000 robotic agents. In swarm robotics, motivations and scenarios are always close to natural counterparts. This is due to the fact that swarms<sup>1</sup> exhibiting all desirable properties (e.g. stability, flexibility, robustness, scalability and simplicity of the agents [7,10,26]) have not yet been built artificially, and thinking in a “swarm-like” way seems to be relatively hard for an organism with a strong emphasis on the individual (like humans are). At the same time, it is relatively hard to re-create mechanisms like those nature uses to create self-organization effects (feedback, positive or negative, or fluctuations) in robotics. For example, chemicals, called *pheromones*,<sup>2</sup> are very often used in nature for swarm-level navigation tasks, exhibiting all the well known self-organization effects. Generation, deposition and detection of chemical substances still pose a great and almost unsolved challenge to a technical system.

Therefore, numerous ways to imitate the concepts that are used by biological swarms have been researched in the past (e.g. the “virtual pheromone”: this can be simulated by a projected light gradient [25], or by robot-to-robot communication [38], or by magnetic footprints [3], or other principles).

<sup>1</sup> Please note that within the “swarm intelligence” community, the term “swarm” is frequently used for systems that biologists would rather call “colony” instead. We will stick to this habit throughout this article.

<sup>2</sup> Pheromones are chemical substances that are emitted by animals to the outside environment. Other animals that perceive these pheromones (even at low dose) react with specific behaviours, e.g. aggregation.

The ability of a single robot to communicate, directly or indirectly, with other members of the swarm, is mandatory in order to establish the cooperative interaction, which is necessary for generating emergent behaviors. This article presents a scenario of collective floor cleaning that has to be performed by a swarm of microrobots. We suggest feasible micromanipulation techniques to grasp obstacles, swarm-level communication by using light pulses and a bio-inspired communication strategy that uses vector information that is passed among the swarm members to navigate the robots in their environment. A suggested robot swarm that implements all these features was simulated and shaped by artificial evolution, showing interesting and surprising features and constraints.

## 3. Hardware features of the suggested microrobot swarm

### 3.1. Communication platform

The ability to sense and to communicate is of paramount importance for large multi-agent systems in which continuous interaction with the environment and neighbors is necessary, in order to explore, perform collective tasks and share information. This last aspect is a capital element both in natural and robotic swarms, where inter-robot communication (direct or indirect) is the base of emergent behaviours. In order to realize such communication capabilities in microrobotic swarms, an integrated, miniaturized, low power communication (and sensing) system is crucial.

The original approach for developing swarm communication strategies and the related hardware tends to biomimicry. Nature offers plenty of examples of colonies of insects and flocks of other animals, which clearly demonstrate swarm intelligence. In particular, the collective strategies demonstrated by some insects (e.g., ants, bees, wasps and termites) have been targeted as the most interesting examples to be imitated. These strategies include decentralised colony homeostasis [43], dynamic regulation of division of labour [6,9,50] and collective selection of feeding sites and nesting sites [44,45,47,49]. It depends not only on the small size, comparable with our microrobot concept, but also on the lower intelligence and complexity of the single unit, which is more likely to be emulated, both from the viewpoint of capabilities and of computational power.

Communication is strongly related to the microrobot size and power available onboard. The first implies that only highly miniaturized communication systems can be integrated, while the latter imposes strict limits on communication distance capability.

There are several examples of wireless techniques for inter-robot communication in multi-agent systems. Radio frequency (RF) and optical communication have been so far the most applied solutions. RF communication has been extensively used down to the range of one-centimeter large robots [11], in a frequency band ranging from 30 MHz to 3 GHz. One of the main problems related to the integration of RF systems on very small robots (millimeter range) is related to the required

antenna size which is able to receive the signal. Antenna scales with  $\lambda/2$  (where  $\lambda$  is the wavelength of the electromagnetic signal). In order to reduce antenna size in the millimeter range, RF transmission around 30 GHz would be required. Other drawbacks of RF communications are related to the lack of directionality and to the relatively large space required for electronics integration.

Optical communication can be a valid alternative especially when the robot size is limited [29]. Infra Red (IR) optical communication and sensing in multi-agent robotic systems have also been demonstrated for miniature robots [11,53]. Optical systems also offer to the robot the capability of detecting external objects, thanks to the high directionality properties of the emitted signal. Directional communication is also of crucial importance for autonomous microrobots in order to understand the reciprocal position in the swarm. On the other hand, the advantage of the directionality also has a drawback in comparison to RF systems, because line-of-sight is required.

Due to the high level of miniaturisation of the I-SWARM microrobots (about  $2 \times 2 \times 1 \text{ mm}^3$ ), the possibility to integrate different capabilities in a single and simple system is highly desirable in order to save space. An optical system can be applied both as a sensor and as a communication tool. Technological issues involve not only power and size limits, but also the realization of fabrication processes for mass-production and for the assembly of chip-scale systems with high functional densities. Optical communication needs at least the integration of an emitter, i.e., a LED or a LASER, and a receiver, i.e. a photodiode. In commercial systems the package encapsulating these devices allows not only a proper positioning and directionality, but it can also provide a light focusing system based on integrated lenses. All these features must be reproduced while designing the integrated custom photonic chip for the I-SWARM microrobots.

In order to allow an automatic and mass fabrication process and to keep the thickness of the whole robot as small as possible, a surface mounting or integration of the devices is necessary. The basic approach is to design a system that can be realized with mass fabrication processes, in order to produce a relatively large number of microrobots at reasonable costs.

Due to these considerations, the system concept needs to be very simple. It consists of a substrate of about  $2 \text{ mm} \times 2 \text{ mm}$  (which could be silicon or a flexible printed circuit board), where LEDs and photodiodes are placed and electrically connected. Each side on the top surface of the substrate hosts one LED die and two close photodiode dies. The structure is particularly conceived in order to have side-directionality in communication (Fig. 1).

A light guiding system and, eventually, microlenses are necessary in order to focus towards other robots a desired light radiation pattern emitted by the microrobots. Concerning this point, two issues are very important:

- focusing light in order to reach higher power density in the emitted beam, since power limits are very strict in miniaturised machines where small spaces can be located for batteries;

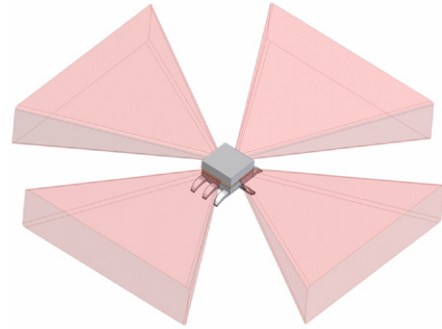


Fig. 1. A realistic emitted-light radiation pattern.

- the wider is the emitted beam, the larger is the covered area during transmission and, consequently, the larger is the probability that information can be received by surrounding robots.

A compromise between these two aspects is necessary. The required architecture should allow not only an optical omni-directional communication between microrobots, but also detection of the presence, position and orientation of surrounding robots. During communication each LED on a single robot is identified by a particular bit string (i.e., for four LEDs, two-bit strings are enough: 00, 01, 10, 11), which is included in the transmitted bit string for high level communication. This technique allows receiving microrobots to understand not only the position but also the relative orientation of the transmitting microrobots. The distribution of photodiodes around the microrobots allows a comparison of the received light intensities of a same signal, thus allowing a more accurate detection of the position and orientation of the transmitting robot. A strategy that allows both collision avoidance between microrobots and a cooperative behaviour without any external supervision can be realized on the base of this method, as illustrated in the following.

### 3.2. Electrostatic micromanipulation in swarm microrobotics

With the enhancements in microfabrication technologies and the growing number of applications in microrobotics, the demand for simple and reliable techniques for micromanipulation is rapidly increasing. This demand is also more important in swarm microrobotics where the transformation of a swarm intelligence architecture into a swarm of microrobots relies just on the possibility to perform active work, to move, and to interact with the environment. It is a matter of fact that when the objects to be handled are smaller than one cubic millimeter, adhesive forces start to overcome gravitational forces [17]. Several research groups are trying to develop reliable micromanipulation techniques in order to perform pick and place tasks with spherical objects a few tens of micrometers in size. In [40] a complete model for micromanipulation using adhesion forces is introduced. The same group described [21] a reliable micromanipulation strategy based on controlled rolling, with the drawback of a high demand of computational power. Other examples, as well as dedicated models for the adhesion forces,

can be found in [33]. The most relevant example of collaborative robotic micromanipulation has been presented in [16].

Although a lot of work has been devoted to manipulation by using adhesion forces, a reliable and repeatable strategy with low computational requirements has not been demonstrated yet. Since the final aim of this work is to design and realize simple manipulation tools for a swarm of mm<sup>3</sup> robots, the micromanipulation strategy has to satisfy both the requirements of reliability and low cost in terms of energy and computational capabilities. In order to pursue this goal, the authors have merged two different approaches to micromanipulation: first, to perform the task in a dry environment in order to reduce the adhesive forces due to humidity; second, to take advantage of electrostatic forces for both grasping and releasing objects. The power consumption required for electrostatic manipulation is almost negligible, since electrostatic forces are established just by imposing a voltage, without any current flow.

An experimental study about forces at the microscale in a controlled environment has been reported in [12]. The same research group set up a microassembly system inside an environmental controlled chamber and performed pick and place experiments by using traditional two-fingered microgrippers. The results of these experiments are reported in [52] as a function of humidity and temperature. Concerning electrostatic manipulation of microobjects by using Coulomb interactions, a precise modeling of object releasing is reported in [48] and the results obtained applying this model are described in [42].

### 3.2.1. Theory and models

When two bodies  $i$  and  $j$  come into contact, the *adhesion* forces [23] are mainly a result of:

1. *Van der Waals* forces, due to intermolecular interactions and influenced by object geometries and materials. The dependency upon the materials is expressed via the Hamaker constant  $A_{ij}$ .
2. *Capillarity* forces, due to the Laplace pressure which takes place in the water meniscus between contacting surfaces. This pressure depends on the liquid surface tension and on the curvature radius of the meniscus.
3. *Electrostatic or Coulomb* forces, due to interactions between charged parts or when a charged particle interacts with a flat surface without electrostatic charge.

The humidity level plays a fundamental role for the first two components of adhesion forces. As the concentration of water in the environment increases, two effects occur:

1. A decrease of the Hamaker constant, thus a lowering of the *Van der Waals* forces in agreement with the theory formulated by Lifshitz in 1956. The dependency of the Hamaker constant on the humidity level is experimentally analyzed in [1].
2. An increase of *Capillarity* forces due to an increase in the number of asperities where a water meniscus forms. A detailed model and several experimental results are reported in [2].

For microscale objects, adhesion forces have larger magnitudes than gravitational forces and they are mainly attractive. Moreover they are proportional to the inverse square or cube of the distances between the objects, thus their influence becomes relevant in the contact regime. Consequently a peculiar threshold of force, commonly referred to as “*pull off*”, has to be overcome to separate two objects. In the case of a sphere of radius  $R$  (object  $i$  in the following) on a planar surface (object  $j$  in the following), the *pull off* force expression is given by the Johnson–Kendall–Roberts (JKR) [24] contact model for the lower boundary or by the Derjaguin–Muller–Toporov (DMT) [15] contact model for the higher boundary:

$$\frac{3}{2}\pi RW_{ij} \leq F_{\text{PullOff}} \leq 2\pi RW_{ij} \quad (1)$$

where  $W_{ij}$  is the energy per unit contact area considering the two surfaces of the objects  $i$  and  $j$  that are in contact.  $W_{ij}$  is expressed as  $W_{ij} = \gamma_i + \gamma_j - \gamma_{ij} = 2\sqrt{\gamma_i\gamma_j}$  with  $\gamma_{ij}$  the interfacial energy,  $\gamma_i$  and  $\gamma_j$  the surface energy of the objects  $i$  and  $j$ . The JKR model fits well when the surface forces are short range in comparison to the elastic deformations they cause (i.e. compliant materials, strong adhesion forces, large tip radii). The opposite limit (i.e., stiff materials, weak adhesion forces, small tip radii) is better described by the DMT contact model. In [31], a model that bridges these two extreme cases using the transition parameter  $\lambda$  is reported.

The dependency of the *pull off* force on the humidity level of the environment is included in the work of adhesion between the two objects. As reported in [54], if the humidity level increases from 5% RH up to 90% RH, measured adhesive forces first decrease until 10% RH is reached, and then slowly increase. This behaviour can be explained by considering that in a dry environment the *Van der Waals* contribution is dominant on capillary forces, thus, as the RH grows, the Hamaker constant decreases and the total adhesive forces become smaller. If the humidity level continues to grow, then capillary forces become dominant over the *Van der Waals* forces, and an increase of total adhesive forces can be observed. The value of total adhesive forces in a 10% RH environment is around half of the one measured in air atmosphere, which typically ranges from 70% RH to 90% RH.

In order to pick up an object from the substrate, a force larger than  $F_{\text{PullOff}}^A$  – evaluated for the particular object in contact with the substrate – has to be applied from the object to the grasping tool direction (Fig. 2(a)). Then, once the object has been grasped and moved onto the target position, the *pull off* force that has to be overcome in order to release it is the force that makes the object stick to the grasping tool,  $F_{\text{PullOff}}^B$  (Fig. 2(b)). Thus, a force that goes from the grasped object down to the target substrate has to be generated and applied. For both the grasping and releasing tasks, electrostatic forces ( $F_{\text{Coulomb}}$  in Figs. 2(a) and 2(b)) can be exploited to overcome the *pull off* force, as modeled and demonstrated just for the releasing phase in [48] and [42].

The voltage which has to be applied, both for grasping and releasing tasks, has the same sign and the same typical amplitude, because of the symmetry of the capacitor system

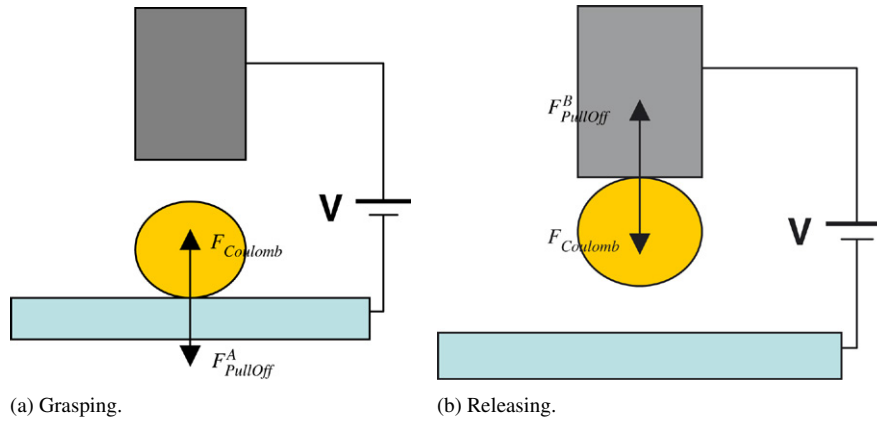


Fig. 2. Schematic illustration of forces during electrostatic grasping (a) and releasing (b) tasks.

tip–object–substrate. Mathematical modeling can be carried on considering the following three components of the system:

1. a cylindrical and conductive manipulation probe with radius  $R_m$  and a length  $L_m$  which is integrated in each microrobot of the swarm;
2. a spherical conductive particle with radius  $R_s$ ;
3. a conductive substrate plate connected to ground potential, where microrobots can move on.

It can be assumed that the spherical particle has a punctual contact with the substrate before grasping and with manipulator before releasing by the adhesion phenomena.

The boundary element method (BEM) has been used in [48] to evaluate the forces generated by electrostatic interactions in the releasing task. The Coulomb force is deduced to be proportional to the square of applied voltage. The force is found to depend on the relative shape of the system, while it does not depend on its size, i.e.

$$F_{\text{Coulomb}} = \{\text{relative\_shape\_factor}\}V^2.$$

Furthermore, the Coulomb force exhibits a peak when the radius of the cylindrical electrostatic tool  $R_m$  is nearly equal to  $R_s$ . This effect is caused by the minimization of the distance between the charge at the corner and the charge on the surface of the sphere, thus yielding maximal (repulsive) Coulomb force. Moreover, as the distance  $D$  between the object and the substrate becomes smaller than  $R_s$  by going to zero, the Coulomb force approaches an asymptotic value that does not depend on the tool length  $L_m$ . In these conditions the following equation is valid:

$$F_{\text{Coulomb}} = \frac{\pi \epsilon_0}{D/R_s} V^2. \quad (2)$$

Since the adhesion force can be estimated by using Eq. (1) and the separation force generated by Coulomb interaction can be calculated by using Eq. (2), the voltage required for detachment can be obtained by the following inequality:  $F_{\text{Coulomb}} > F_{\text{PullOff}}$ .

Therefore, by using the higher boundary for the *pull off* force, the voltage required for detachment can be written as:

$$V > \sqrt{2W_{ij} \frac{D}{\epsilon_0}} \approx 5.49 \times 10^5 \sqrt{W_{ij} D}. \quad (3)$$

For practical surfaces, having some roughness or contamination,  $W_{ij}$  can be assumed in a range between  $0.01 \text{ J/m}^2$  and  $1 \text{ J/m}^2$ . Thus, the voltage required for detachment can be expressed as:

$$V > 5.49 \times 10^{4 \dots 5} \sqrt{D}. \quad (4)$$

For a typical gap of  $5 \mu\text{m}$  between object and probe, the theoretical voltage needed in order to obtaining releasing ranges between 120 V and 1200 V. Obviously, the voltage should be also calculated in consideration of the electric discharge and tunnelling current.

Experimental results that validate this theoretical approach are reported in [42]. The voltage applied between the manipulation probe and the substrate plate was measured when the spherical microobject was detached from the probe tip. The experiment was performed in air atmosphere. Typical voltages needed in order to obtain detachment of a  $15 \mu\text{m}$  radius solder ball ranged between 100 V and 500 V. These large values, obviously not suitable for microrobotic applications, are mainly due to the capillary interaction forces present in a normal air atmosphere environment. Thus, by reducing the humidity level in the range of 10% RH, it would be possible to demonstrate releasing applying lower voltage values. In particular, assuming a decrease to half the value of the total adhesive force, as reported in [54], it is possible to expect that the voltage needed to obtaining releasing would range between 70 V and 350 V.

The same micromanipulation strategy can be used also for picking up a spherical object: in this case, the Coulomb force has to overcome the *pull off* force due to the contact between the spherical object and the substrate. Consequently, the same theory and the same models still apply.

In order to verify the effect of humidity on the results obtained in [42] and to validate if the Coulomb interactions can be used also for grasping tasks, several experiments have been performed in a humidity controlled environment. In the

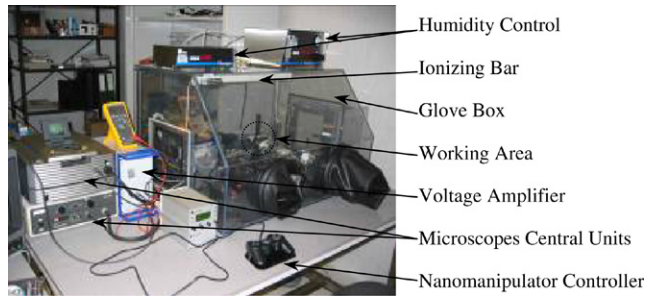


Fig. 3. Micromanipulation setup.

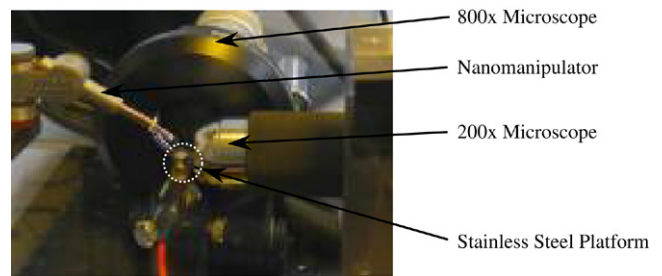


Fig. 4. Enlarged view of the working area.

following sub-paragraphs the experimental setup is described and the results are discussed and analyzed, in order to prove the feasibility of the electrostatic manipulation strategy in swarm microrobotics.

### 3.2.2. Experimental setup description

A full micromanipulation setup has been set up inside an environmental controlled chamber (Terra Universal Inc., Series 100 Polymer Glove Box) illustrated in Fig. 3. The Glove Box is equipped with a humidity sensor (Terra Universal Inc., NitroWatch) which provides a continuous readout of the internal humidity level and operates together with a control system (Terra Universal Inc., Dual Purge) to automatically maintain the desired internal humidity level. The control system regulates the nitrogen flow into the chamber, thus allowing us to conduct experiments with a controlled humidity in the range of 0...100% RH, with an accuracy of  $\pm 3\%$  RH. An ionizing bar is also integrated into the system in order to neutralize the static charges in the working area.

The working area (Fig. 4) is observed laterally from two sides by using two fiber optic microscopes, mounted perpendicularly: VH5901 with  $200\times$  magnification from Keyence (Woodcliff Lake, NJ, USA) and KH2700 with  $800\times$  magnification from Hirox (Tokyo, Japan). The Hirox has capabilities of on-line distance measurements, thus making possible the estimation of distance between the needle and the object to be grasped. The manipulation needle is mounted on a 3 d.o.f. commercial nanomanipulator (Kleindiek Nanotechnik GmbH, MM3A), equipped with three piezo-motors (one motor for each d.o.f.) with nanometric step resolution. The tool is a  $26\ \mu\text{m}$  in diameter cylindrical wire made by aluminium (Fig. 5) electrically connected to a signal generator through a voltage amplifier. The ground of this applied potential is connected to a stainless steel platform where the object to be grasped is located. Conductive solder balls (Sn: 96.5%, Ag: 3.5%) with radius ranging from  $15\ \mu\text{m}$  to  $25\ \mu\text{m}$  have been selected as spherical microobjects. The platform has a diameter of 6 mm; thus it can be considered as an infinite plane if compared to the object to be grasped (the ratio between a solder ball and the platform is typically 1:300).

### 3.2.3. Experiments description and results

Grasping and releasing experiments by using electrostatic force have been carried out in a humidity controlled atmosphere. During these experiments the following protocol has been used:

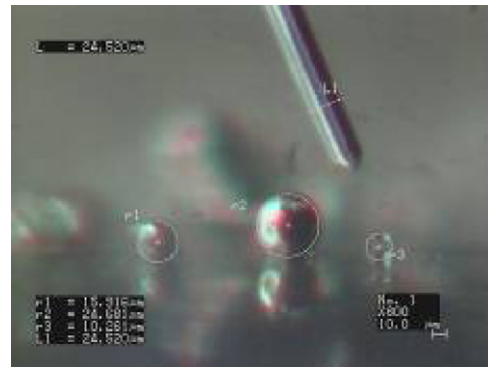


Fig. 5. Aluminium grasping tool and different spherical objects to be grasped.

- The stainless steel platform has been cleaned with an ultrasonic bath in order to remove dust and debris;
- Solder balls, separated from the flux medium by using isopropyl alcohol, have been placed on the platform;
- The stainless steel platform has been mounted in the manipulation system and connected to ground ( $V = 0$ );
- The experimental setup has been sealed inside the environmental controlled chamber and the desired relative humidity has been imposed by injecting nitrogen in the glove box;
- The target ball has been selected by using both images of the two microscopes;
- The electrostatic tool has been moved by the nanomanipulator closer to the target ball;
- Grasping tests have been performed by varying the applied voltage on the tip of the tool and the distance between the tool and the spherical object;
- Once the object has been grasped, releasing tests by electrostatic force have been performed; a constant gap of  $5\ \mu\text{m}$  between the object and the platform has been fixed and the electrostatic voltage has been increased until the release occurred.

In order to grasp the object, the electrostatic force  $F_{\text{Coulomb}}$  has to overcome the *pull off* force due to the adhesion at the interface between the stainless steel platform and the object itself. Experimental evidence demonstrates that, if the voltage remains below 50 V, the pure Coulomb force is not enough to grasp the object, even if the relative humidity is reduced down to 10%. Maybe this limitation can be overcome by optimizing the shape of the tip, since this is an important parameter that influences the magnitude of  $F_{\text{Coulomb}}$ , as explained above.



Fig. 6. A 23 μm spherical object before (a) and after (b) grasping by using 20 V with a relative humidity of 10%.

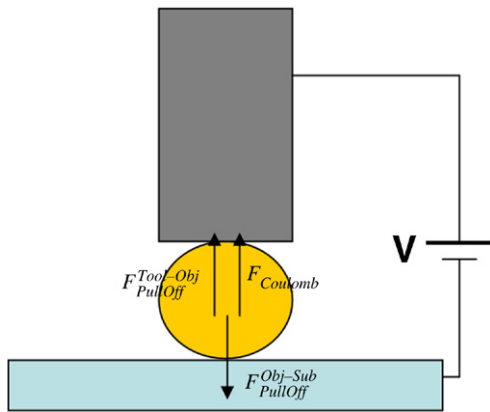


Fig. 7. Schematic illustration of forces during electrostatic grasping, when the tool touches the object.

In order to lift the object, a contact between it and the tool has to be established. With this configuration the *pull off* force of the interface “tool – object” works in synergy with the attractive Coulomb force (Fig. 7). Thus the inequality to be satisfied in order to lift the object becomes:

$$F_{\text{Coulomb}} + F_{\text{PullOff}}^{\text{Tool-Obj}} > F_{\text{PullOff}}^{\text{Obj-Sub}} \quad (5)$$

By using this strategy, grasping has been achieved all the times, with a minimum grasping voltage ranging from 20 V to 30 V for 10% relative humidity (Fig. 6). The grasping voltages in these environmental conditions versus the radius of the grasped object are plotted in Fig. 8. Tests with different humidity conditions (i.e. 30% and 50% RHs) have also been performed and the recorded grasping voltages are plotted in Fig. 9. The results are in agreement with [54], demonstrating that the optimal condition to perform electrostatic grasping tasks can be achieved in a 10% RH environment. Another interesting result is that the radius of the object to be grasped does not really influence the grasping voltage. An explanation for that can be found in the small dimensions of the objects, that make the gravitational force negligible if compared to adhesion effects.

Melting of the sphere (15 μm radius) on the tip of the tool has also been observed for an applied voltage of 70 V (see Fig. 10).

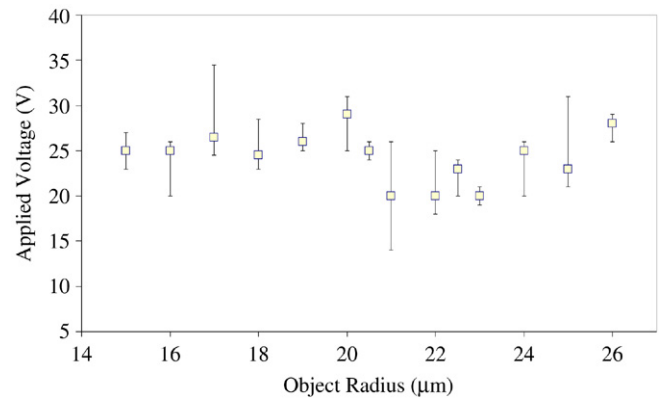


Fig. 8. Grasping voltage versus radius of the object for a relative humidity of 10%. The plot shows the average of the grasping voltage for five-times measurements.

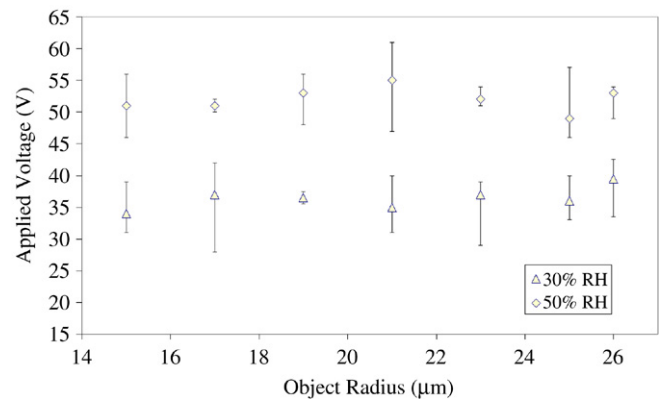


Fig. 9. Grasping voltage versus radius of the object for a relative humidity of 30% and 50%. The plot shows the average of the grasping voltage for five-times measurements.

Concerning electrostatic releasing, experimental data show that, with a relative humidity of 10% and a gap distance of 5 μm (Fig. 11), a voltage ranging from 37 V to 47 V is required in order to release the object from the grasping tool. The distance between the solder sphere and the stainless steel platform has been evaluated as half of the distance between the spherical object and its reflected image. The releasing turns out to be highly reliable and repeatable. Moreover the required voltage for releasing in a 10% RH atmosphere is found to be even

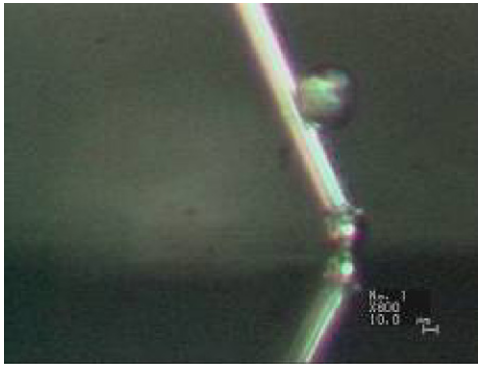


Fig. 10. Spherical object melted to the tool for an applied voltage of 70 V.

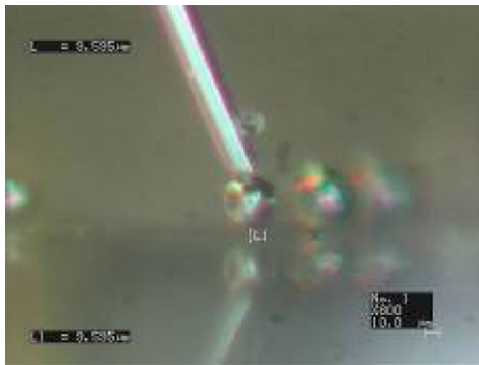


Fig. 11. Releasing experiment starting from a gap of about  $5\ \mu\text{m}$  between the object and the platform.

smaller of what expected from theory (from 37 V to 47 V instead of 70 V).

#### 4. Software features of the suggested microrobot swarm

##### 4.1. Collision avoidance strategy

In a typical swarm scenario, microrobots walk often randomly. In the proposed strategy they frequently stop in order to emit some light impulses. Because of power limitation, the LEDs will be serially activated and each robot will keep all photodiodes off, except those on the front side of the robot in order to detect an obstacle. The detection threshold of photodiodes defines the range of the signalling for a fixed power. Surrounding robots can detect not only the presence and position of one or more other robots, but also understand if it/they are on a direct collision course: the particular LED-codes received inform the robots about the walking direction of the transmitting robot. If a collision route is detected, other microrobots will simply turn and go towards the opposite direction of the detected light. Stability and convergence issues in crowded zones have been investigated through computer simulations and they will be presented in the following. Preliminary results have shown that one of the biggest problems with robot swarms is the clustering of colliding robots. To lower the negative effects of such traffic jams, we implemented an additional Boolean flag that was added to the collision-avoidance signal emitted by the LEDs. Robots emitting this signal have higher repellent forces in the potential-fields that

are used for collision avoidance, thus giving these robots a sort of priority movement in deadlock situations. In our simulation platform, such signals can be emitted by scouts and by loaded robots. For further descriptions of these robot states, see below.

##### 4.2. The swarm scenario

The first application we designed for the presented hardware of the microrobot swarm is a scenario of “collective arena cleaning”. Initially, the arena is filled with hundreds of equally distributed robots that are oriented randomly. Two areas contain dust particles; we will refer to these areas as “dust areas” further on. In the centre of the arena, the designated “dump” area is located. The goal of the robot swarm is to collectively clean the arena by picking up the dust, by carrying it over to the dump area and by dropping the dust particles there. The scenario shall be performed by a robot swarm of a size of up to 1000 robots.

The constraints for the robot swarm are the followings:

1. A robot can detect the presence of a dust particle only if it is located directly beside/beneath it. The robots have thus no long-distance sensing for dust.
2. Also the location of the dump cannot be detected on a long range. The robots can only detect whether they are already located at the dump area or not.
3. The robots can communicate via their LEDs for a distance of just 3–4 robot-diameters.

Considering these constraints, an optimal robot strategy would be:

1. The robots should compensate for their limited dust/dump-sensing abilities by using their robot-to-robot communication for advertising the location of the dust areas and the location of the dump area.
2. The robots shall draw advantage from the big size of the robot swarm and use the mass of robots to constantly search the arena for possible cleaning sites.
3. The robots can carry the dust, but there is the risk of dropping the particle. So the transport of the particles shall be performed on the most directed way, thus minimising the transportation time.

To investigate this swarm scenario, the LaRoSim V0.42 (large<sup>3</sup> robot-swarm simulator) simulation platform has been used. The details of this platform are given in [46]. The simulator is a multi-agent simulator that simulates hundreds or thousands of robots within an arena. It is implemented in NetLogo 3.02 [51]. The simulator incorporates the communication principles described above (4 LEDs, 4 photodiodes). Fig. 12 shows a screenshot of the simulator at runtime. The simulator also allows one to simulate noise in communication, by assigning a given amount of error on distance measurements, on communication and on sensing.

##### 4.3. The “vector-based” communication strategy

The cooperative strategy among the microrobots is based on the following steps. Referring to Fig. 13(a), where robot 1 has

<sup>3</sup> The term “large” refers to the size of the robot swarm NOT to the size of a single robot.

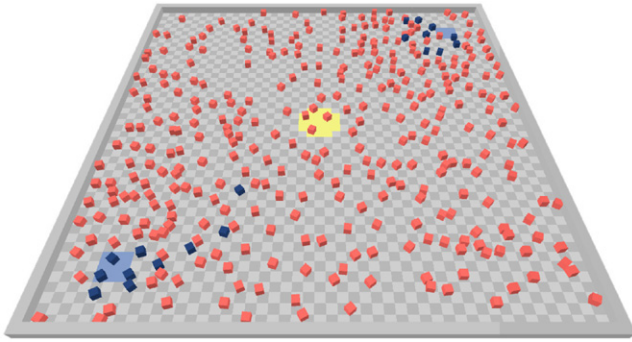


Fig. 12. A screenshot of the LaRoSim simulation platform. The screenshot shows the typical “cleaning”-scenario simulated within this platform: The two blue-coloured floor areas represent “dusty” areas that have to be cleaned by the robot swarm autonomously. Empty robots (red boxes) head towards these areas. As soon as they pick up a dust particle they are coloured in blue. These loaded robots then head towards the yellow dump area to drop the particle there. (For interpretation of the references to colour in this figure legend, the reader is referred to the web version of this article.)

found a target and robot 2 has entered its communication range. In a more general configuration, robot ( $N + 1$ ) needs to know:

- A. The relative direction of robot  $N$  (automatically understood in signal detection);
- B. The relative orientation of robot  $N$  (received by bits communication);
- C. The target direction vector as regards robot  $N$  (received by bits communication).

Combination of points B and C transposes the vector of the target from the reference of robot  $N$  to the reference of robot ( $N + 1$ ). In this way the vector called  $V$  in Fig. 13(a) is acquired from robot ( $N + 1$ ) relative to its own reference system. The final vector ( $V_F$ ) for the target direction is obtained by doing a vector sum of the components of the calculated vector  $V$  and the vector  $V'$  (expressed by point A). This allows each robot to know both the direction and the distance to the target. In Fig. 13(b) an example of the propagation of this strategy to several members of the swarm and the formation of the vector trail are represented (the vector length is arbitrary). This strategy allows broadcasting the information within the swarm, creating a pattern which will extend in time, thus increasing progressively the probability that other microrobots could meet it and, therefore, receive information. In our simulations we assumed error in communication and we

took account for the fact that the robots will not be able to detect the correct angle to neighboring robots. In our simulations, the robots were able to exploit directional information only at a very low level by evaluating the position of the photodiode that received the communication. One example: If a robot receives communication from a neighbor that is located  $112^\circ$  (always counted clockwise;  $0^\circ$  represents the front of each robot), the receiving focal robot only “knows” that the message comes in by the right photodiode and assumes the sender’s position at  $90^\circ$ . Of course, this leads to additional errors that enter into the system, as these vectors are passed on and are accounted by other robots in their vector calculation. In addition to that, we allowed only one communication channel per photodiode, regardless of how many robots were located within the light beam cone of  $60^\circ$  opening angle. Communication was restricted to the nearest neighbor in this case. It is worth noting that the robots always communicate two type of vectors simultaneously: one pointing to a dust area and one pointing to the dump area. Empty robots move along the first vector while loaded robots move along the latter one.

#### 4.4. General simulator settings

Table 1 gives the parameter settings used in LaRoSim for the simulations reported in this paper. In that table are listed those parameters that are not optimised during artificial evolution. In particular the fixed (not evolved) parameters reflect the hardware constraints, the arena settings and the assumed level of error within the system. Spatial values are given by the robot-diameter (rd) to keep our simulator scalable with robot size.

#### 4.5. Introducing negative feedback and fresh information into the system

So far, only a positive feedback loop has been described. Robots that get informed about their targets start to move towards these goals. They communicate these targets again to their neighbors. This system leads to aggregation of robots at their target places. But without any negative feedback, old and outdated information cannot leave the system. As described above, errors can accumulate as a vector gets communicated multiple times among the robots. In addition, information can become outdated, for example when a dust-area is fully cleaned up. In this case vectors that are still pointing towards this

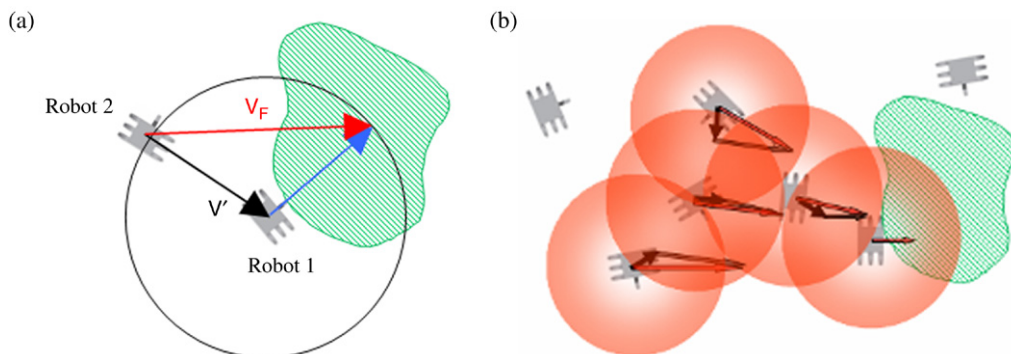


Fig. 13. (a) Vectorial sum for target direction reconstruction. (b) An example of the swarm formation induced by vector propagation within a group of 5 robots.

Table 1  
Default parameter settings used in the simulation experiments described in this article

Parameter	Value
Arena-size	49 × 49 rd
Dust-particles	72 particles
Robot-speed	0.5 rd/step
Error-distance-measure	10%
Error-in-communication	10%
Communication-radius	3.5 rd
Number-of-LEDs	4
Inter-LED-angle	90°
LED-beam-aperture	60°
<i>P</i> (communication-break)	0.1
Communication-capacity	32 bit/message
Dust-in-arena	72 particles

This table gives only those parameters that reflect hardware constraints and arena features. The strategy-parameters, that are shaped by artificial evolution, are described separately. The unit “rd” represents the maximum diameter of one robot.

former dust area should leave the system to avoid useless aggregation of robots at this place. In nature, negative feedback is very important to reduce old information. For example, the pheromones deposited from ants’ tails evaporate over time, honeybees abandon from their feeding places with a given probability and the chemical signals emitted by slime mould amoebas are broken down over time. In addition to reducing the life-time of old information, social insects have evolved techniques to ensure the steady input of fresh information in their foraging systems. Often “scouts” search the environment almost randomly for new feeding sites, neglecting the available information about already known sites. In order to introduce comparable negative feedback and a steady input of fresh information, three additional features into the vector-based swarm strategy have been implemented:

- (1) Use-hop-count: A hop-count to each vector that is incremented with every communication act has been added. By allowing the robots to only update to “younger” information than they already possess, we prevent old information from further spreading within the robot swarm and we intend to keep the robots always “up to date”. If this Boolean parameter is set to TRUE, the robots use this feature.
- (2) p(vector-forget): This parameter determines the probability (floating point value between 0 and 1, triggered every time step) for a robot to forget the vectors it has in memory. It will then be updated by one of its neighbors. This way we intend to shorten the period vectors remain within the system.
- (3) Is-Scout: Robots that have set this flag to TRUE communicate like all other robots and they also detect dust areas and dump areas as usual. But they do not move according to any one of the communicated vectors, thus they will never aggregate. Our intention was that these robots would perform always a random walk and would act as a communication bridge between densely aggregated clusters of robots. In addition, these robots will be more effective in roaming through wide areas of the arena and in

detecting new dust areas. The robots not acting as “scouts” will be called “workers” further on.

In addition to that, we introduced two additional parameters called “weight-find-dust” and “weight-find-dump”, both are floating point parameters between 0 and 1. A weight of 0.5 means that a robot will just follow the vector in 50% of its moves and perform a random move in the other 50% of time steps. The higher the weight is, the more frequently the robot follows the vector. This was added to prevent the robots from “deadlock-situations”. The following sections will investigate the importance of these additions onto the global swarm performance.

#### 4.6. Simulation results

The first goal of the simulations was to find optimal values for the parameters that are associated with the proposed communication strategy and with the robots’ navigation. To achieve this, an artificial evolution (“Evolutionary Strategy”) that lasted for 120 generations with a population size of 10 swarms was performed. It is worth noting that this was “colony-level” selection, as one evolved genome determined the strategy of one whole swarm. In total, 1200 simulations of the cleaning scenario were performed and evaluated during this evolution. The best two individuals (=swarms) of each generation were selected and transferred without any change to the next generation (elitism). The remaining 8 offspring of the next generation were determined by drawing them randomly from the previous generation, whereby the probability of an individual to be selected for reproduction depended on its relative fitness compared to the other swarms. The mutation rate of a “dependent mutation” was set to 0.5; the span of mutation was  $\pm 0.05$  of the parent’s parameter value. The probability of an independent mutation (totally random new parameter value) was 0.05. The chance for a “cross-over”-event was set to 0.2. In 50% of these crossovers, we performed “intermediate crossover”, thus the offspring’s parameter values were calculated by averaging the two parents’ parameter values. In the other 50% of crossovers, the values of one of the two parents were transferred to the offspring.

For assessing a swarm’s fitness, the following fitness function was created: For every dust item a swarm delivered at the dump, 40 fitness points was achieved by the swarm. For every dust item that was picked up but not delivered, 20 fitness points were achieved. Each collision between two robots was counted and reduced the fitness gain by 0.05 divided by the number of robots. Each simulation run lasted for 800 time steps. If the swarm delivered all 72 dust particles within this time, an extra bonus was achieved: For every time step of early finishing, 10 additional fitness points were achieved. This leads to the following maximal fitness values:

- (1) Unsuccessful swarms that are swarms that do not deliver all dust items at the dump can achieve a maximum fitness measure of 2860 points. This threshold is indicated by the dashed line in Fig. 14(a).

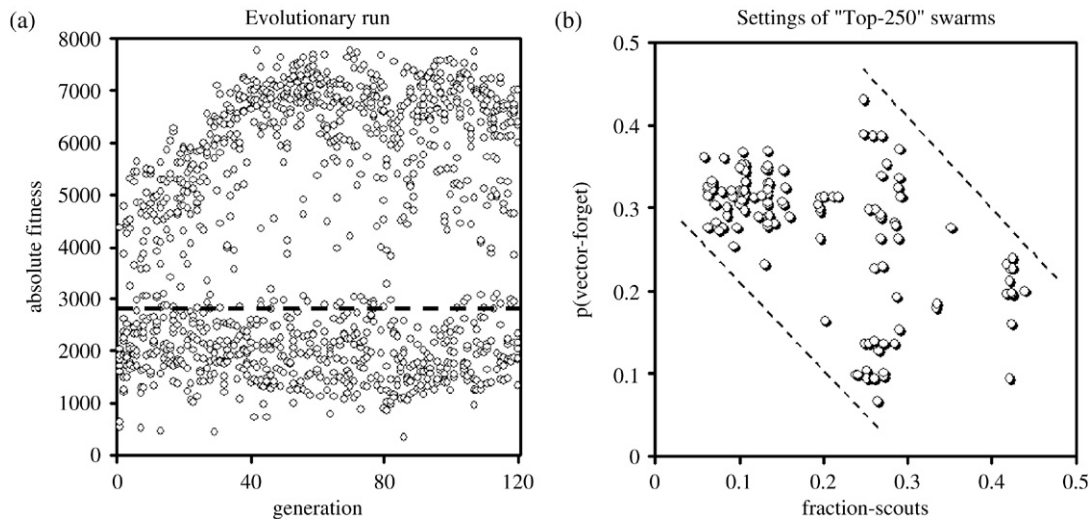


Fig. 14. (a) Results of the “Evolutionary Strategy”. Throughout 120 generations, more-and-more effective swarms evolved, what is expressed by the absolute fitness. The dashed line indicates the maximum amount of fitness points a swarm can achieve without removing all dust particles in the arena. In total, 1200 simulation runs are depicted in the left subfigure. (b) Two related parameters,  $p(\text{vector-forget})$  and  $\text{fraction-scouts}$ , that evolved in specific combinations. This subfigure shows the 250 fittest swarms that evolved between generations 35 and 100 (the “plateau” in the left subfigure). The two dashed lines indicate that the 250 best swarms show a negative correlation between these two parameters. Two swarms at the extremes of these settings are depicted in Fig. 16 at runtime.

- (2) Successful swarms, that are swarms that manage to deliver all 72 dust items during the allowed 800 time steps, can reach higher values. Assuming a theoretical shortest finishing time of approximately 250 time step, this results in an absolute maximum of 8360 fitness points, assuming zero collisions.

#### 4.6.1. Evolution of optimized robot swarms

As can be seen in Fig. 14(a), the swarms evolved quite quickly. Between generation 1 and generation 35, a steady increase of the absolute fitness of the best swarms is clearly visible. Nevertheless, a high fraction of swarms was not very fit and did not achieve the final goal. Data analysis showed that 464 out of 525 swarms that did not succeed in cleaning up the whole arena did not account for the vector-associated hop-count; thus these robots did not update themselves by vectors “older” than those they were already carrying. In contrast to that, 655 out of 675 swarms that succeeded did account for this hop-count. This clearly indicates the importance of the parameter setting “use-hop-count=true” for fit swarms.

The fraction of scouts within the swarm was equal in both groups. Successful swarms had a fraction of scouts of  $0.16 \pm 0.12$ ; unsuccessful swarms had a fraction of scouts within the swarm of  $0.16 \pm 0.13$ . The same was found when comparing the evolved values of the parameter  $p(\text{vector-forget})$  for both groups of swarms. Successful swarms had a value of  $p(\text{vector-forget})$  of  $0.28 \pm 0.13$ . Unsuccessful swarms had a value of  $p(\text{vector-forget})$  of  $0.29 \pm 0.16$ .

To additionally test the importance of the parameter “use-hop-count”, we performed an additional simulation experiment. We took the parameters of the optimal swarm that evolved in 120 generations and performed 12 runs with “use-hop-count=true” and 12 runs with “use-hop-count=false”. Simulation runs lasted until the swarms had delivered 66 of the

72 dust particles at the dump area, or until a time limit of 1200 time steps was reached. The results are shown in Fig. 15.

Although the successful and unsuccessful swarms showed no difference in their mean ratio of scouts to workers and in their mean values of  $p(\text{vector-forget})$ , Fig. 14(b) shows interesting statistical facts: When we selected the 250 fittest swarms out from the “plateau”-phase (generations 35–100) and plotted the values of “fraction-scouts” against the values of  $p(\text{vector-forget})$ , we found a strong negative correlation between these two parameters. Fit swarms that had high values in one parameter tend to have low values in the other one. As Fig. 16 demonstrates, the extreme settings accomplish the task in different ways but achieve equivalent fitness this way.

During our evolutionary runs, these two very fit “types” of swarm have evolved. Table 2 shows the evolved parameters of the fittest swarm of each type. This table simultaneously lists the “genome” that was used in the evolutionary strategy. As already mentioned, the first type of swarm evolved a lower ratio of scouts to workers and a higher value  $p(\text{vector-forget})$ , compared to the second type of swarm. The density of the swarm converged to values between 11.8% (280 robots) and 13.2% (314 robots). The biggest swarm that was tested during the evolutionary run consisted of 785 robots. Concerning the collision-avoidance behaviour, both types of swarm represent the same solution: Empty robots tried to keep a distance of 0.40 sr/0.41 sr to robots that showed the “priority signal” (scouts and loaded robots). In addition, empty robots tried to keep a distance of 0.65 sr/0.77 sr to other empty robots. And loaded robots tried to keep a minimum distance of 0.25 sr/0.27 sr to other robots. The unit “sr” means “sensory radius”. The sensory radius was set to 3.5 robot diameters in our simulations. These collision-avoidance settings allowed dense trails of loaded robots heading toward the dump and loose clusters of empty robots and scouts. This is important, because loose formations of scouts and empty robots can roam the arena

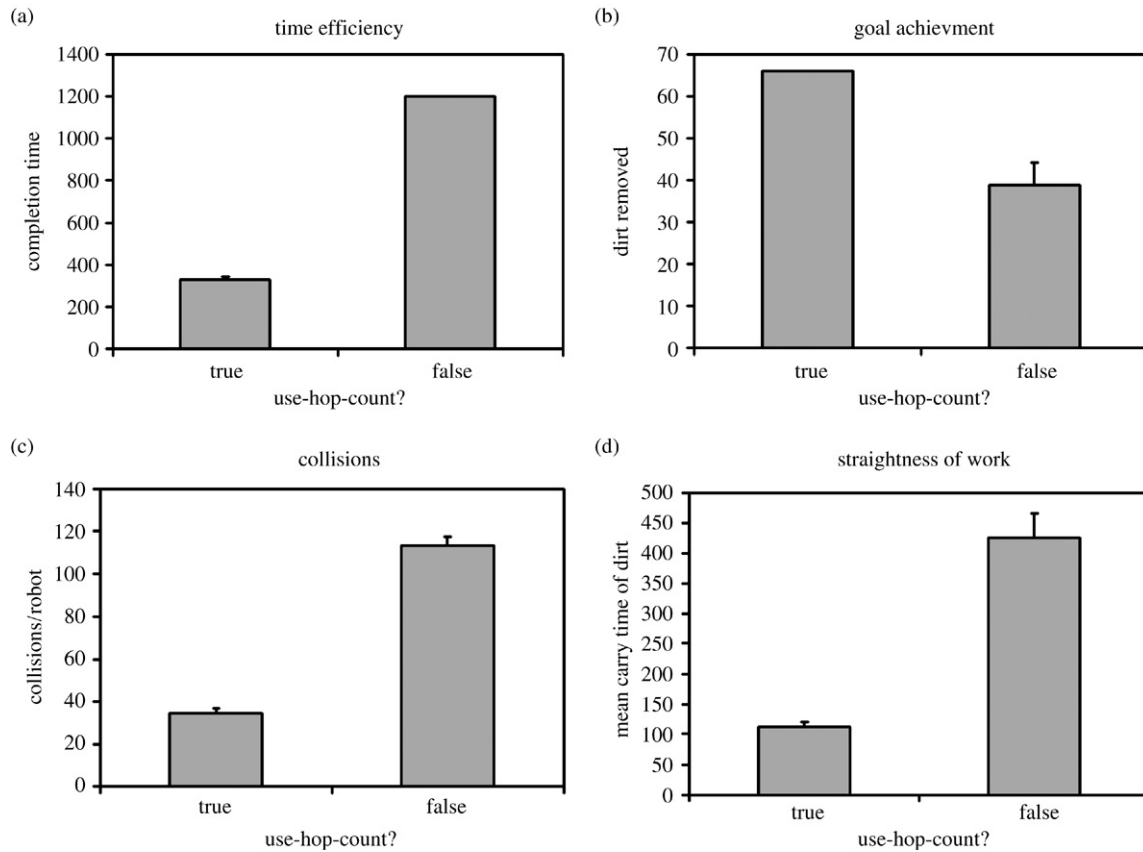


Fig. 15. The importance of the parameter “use-hop-count” for the vector-based strategy. If this parameter is set to TRUE, then the goal is achieved much more quickly (a), more dust is removed (b), fewer collisions happen (c) and the dust particles are carried on a shorter way to the dump area (d). All figures show medians and third quartiles.  $N = 12$  per setting (per bar).

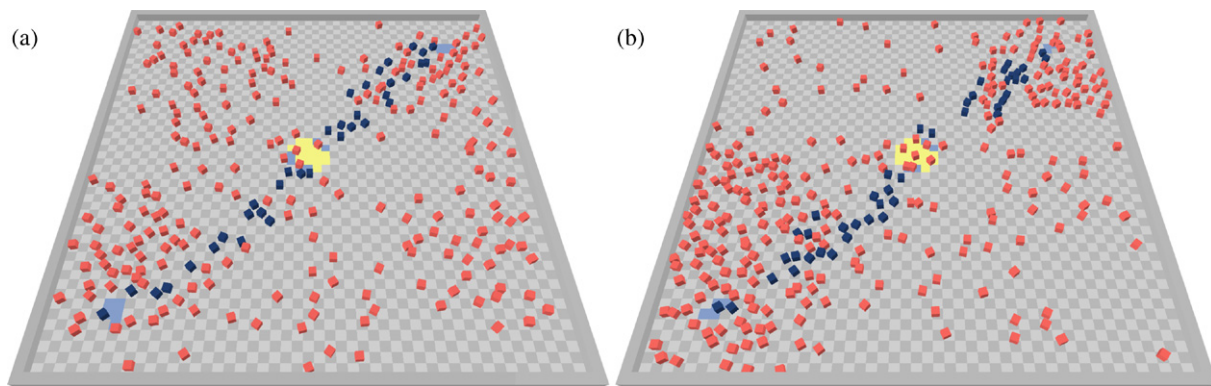


Fig. 16. (a) Screenshot of one type of very fit swarms. This type (type 1) has a low fraction of scouts in the swarm (8%) and a high  $p(\text{vector-forget})=0.29$ . (b) A screenshot of the other type of very fit swarms. This type (type 2) has a high scout-to-worker ratio (27%) and a low value of  $p(\text{vector-forget})=0.14$ . These different parameter settings result in different global behaviour but in the same swarm efficiency, as it was measured by our fitness function. The swarm in the right figure shows a more intensive aggregation of empty robots around the dust areas, the left swarm builds several “sub-swarms” that are narrowly connected.

better to find new dust and can be easily “penetrated” by the trail of loaded robots.

As can be seen in Table 2, the artificial evolution turned off the priority signal of scouts but turned on the priority signal of loaded robot, a fact that helped to form the solid trails of loaded robots heading towards the dump area. Also the “weight-find-dump” was significantly higher than the “weight-find-dust” in both types of very fit swarm, again allowing a direct trail from dust to dirt.

#### 4.6.2. The optimal density of the robot swarm

The density of robots is a crucial topic for swarm robotics. If swarm densities are too high, robots collide too frequently and traffic jams arise, that can lead to clusters of robots that cannot achieve their goals anymore. Too low densities of robots lead to breaks in the communication bridges and prevent important information from spreading throughout the entire swarm. We took the parameters described in Table 1 and in the left column of Table 2 as default settings and performed simulation runs

Table 2  
The parameters that evolved during our Evolutionary Strategy

Parameter	Type 1:	Type 2:
Absolute fitness	7771 points	7766 points
Density-of-robots	11.8%	13.2%
Fraction-scouts	8%	27%
p(vector-forget)	0.29	14%
Use-hop-count	true	true
Priority-coll-avoid-dist	0.4 sr	0.41 sr
Empty-coll-avoid-dist	0.65 sr	0.77 sr
Loaded-coll-avoid-dist	0.25 sr	0.27 sr
Priority-signal-scouts	FALSE	FALSE
Priority-signal-loaded	TRUE	TRUE
Weight-find-dust	0.83	0.82
Weight-find-dump	0.94	1.00

The table shows the parameter settings of the two swarm types that are displayed in Fig. 16. The unit “sr” refers to the sensory radius of the robots, which was set to 3.5 rd (robot diameters).

with varying densities (0.05–0.4) of the robot swarm. Due to the size of the arena used ( $49 \times 49$  rd), these densities correspond to swarm sizes between 120 and 960 robots. For example: A density of 0.4 characterizes a robot swarm of a size that covers 40% of the area of the arena with robots:  $49 \times 49 = 2401$  possible robot locations,  $2401 \times 0.4 = 960$  robots in the swarm.

The experiments lasted until the robots had delivered all 66 of the 72 dust particles that were located in the arena, or after 1200 time steps, regardless of the number of delivered particles. These experiments were repeated 6 times per setting; the results are presented in Fig. 17.

Concerning the time it took to complete the task, a swarm density between 0.1 and 0.15 was found to be an optimal setting. Swarm densities between 0.1 and 0.2 were able to successfully clean the whole arena. Swarms having densities between 0.1 and 0.15 led to the lowest number of collisions per robot. Swarm densities between 0.1 and 0.15 led to the lowest mean carriage periods per dust particle.

## 5. Conclusions and future work

This paper has illustrated a novel swarm microrobotic platform which takes advantage of the advances in microsystem technologies and micromanipulation in order to give the opportunity to apply swarm intelligent architectures to true miniaturized robotic platforms. This approach can produce a twofold scientific result: It allows realizing a biomimetic platform to better understand the communication and operation strategies of biological swarm systems, and it can produce a real advancement of microsystem and robotic technologies by fostering a new generation of novel components for mobile microrobotics.

The extreme miniaturization of the robotic agents involves the development of a miniaturized and low power communication system to be embedded in each microrobot. An optical multifunctional microsystem  $4 \text{ mm}^2$  in size is currently at the design stage. This architecture should enable further scaling down in addition to the possibility of batch production. The final goal will be the realization of a custom integrated optoelectronic chip, where optoelectronic devices and tracks are realized

in the substrate with standard microelectronic processes or directly in the integrated control chip of the microrobot, through advanced heterogeneous integration processes.

As regards the ability of each robot to perform collaborative microtasks and to operate in the microscale, results obtained from electrostatic grasping and electrostatic releasing experiments allow to conclude that this technique could be successfully applied in order to move spherical conductive objects, with radius ranging between  $15 \mu\text{m}$  and  $25 \mu\text{m}$ , from an arbitrary starting position to a target location on a surface at ground potential. In order to apply this strategy, the micromanipulation equipment consists just of a 2 d.o.f. conductive microtool, connected to a voltage generator. In addition, by working in a humidity controlled environment where 10% RH has been imposed, it is possible to apply electrostatic grasping and releasing by using a voltage level suitable for swarm robotic micromanipulation purposes (ranging from 20 V to 40 V). This voltage level can be generated on board by charging a capacitor up to the desired voltage level and then maintaining it in case of charge leakage. Since no current flow is needed during all the manipulation procedure, it would be possible to implement this micromanipulation technique with negligible costs in terms of power consumption. Additional work will be devoted in designing a new shape of the grasping tip that would increase the Coulomb interactions, in order to further decrease the operative voltage of the electrostatic tool.

The suggested vector-based communication strategy was proven to work efficiently and robust by simulation experiments. In nature, vector information is used by several animal species for navigation. Most prominently, the desert ant *Cataglyphis* is able to find the shortest path back to the nest by vector summarisation [4,14]. But also other animals (e.g., spiders, crabs and honeybees) were found to use vector information for navigation [28,36,41]. But in our swarm scenario, the robots do not only navigate by vector information, they also communicate vector information among swarm members. This ability is only found in honeybees, who communicate vectors to their food targets by performing specific dances on their combs. The discovery of this high-level communication was done by K. v. Frisch, who was awarded a Nobel price for this work [18]. In addition to the navigation and the communication of vectors, specific mechanisms that introduce negative feedback into the system must be added. All examples of swarm intelligence in nature use similar mechanisms to promote new information faster than older information and to force out-dated information to diminish, if it is not reinforced anymore. This can be seen in all pheromone-based communication principles, like it is found in ants, in termites and in honeybees [10]. In this paper this was achieved by implementing a vector-forget rate, a priority communication for fresh information and by adding a dedicated scout caste. The resulting swarm was found to be robust but flexible, scalable and simple, all features that are typically characteristic for “swarm intelligence” [7,10,26]. By performing artificial evolution of the swarm parameters we obtained two different types of swarm that achieved the same goal on different ways by showing the same efficiency.

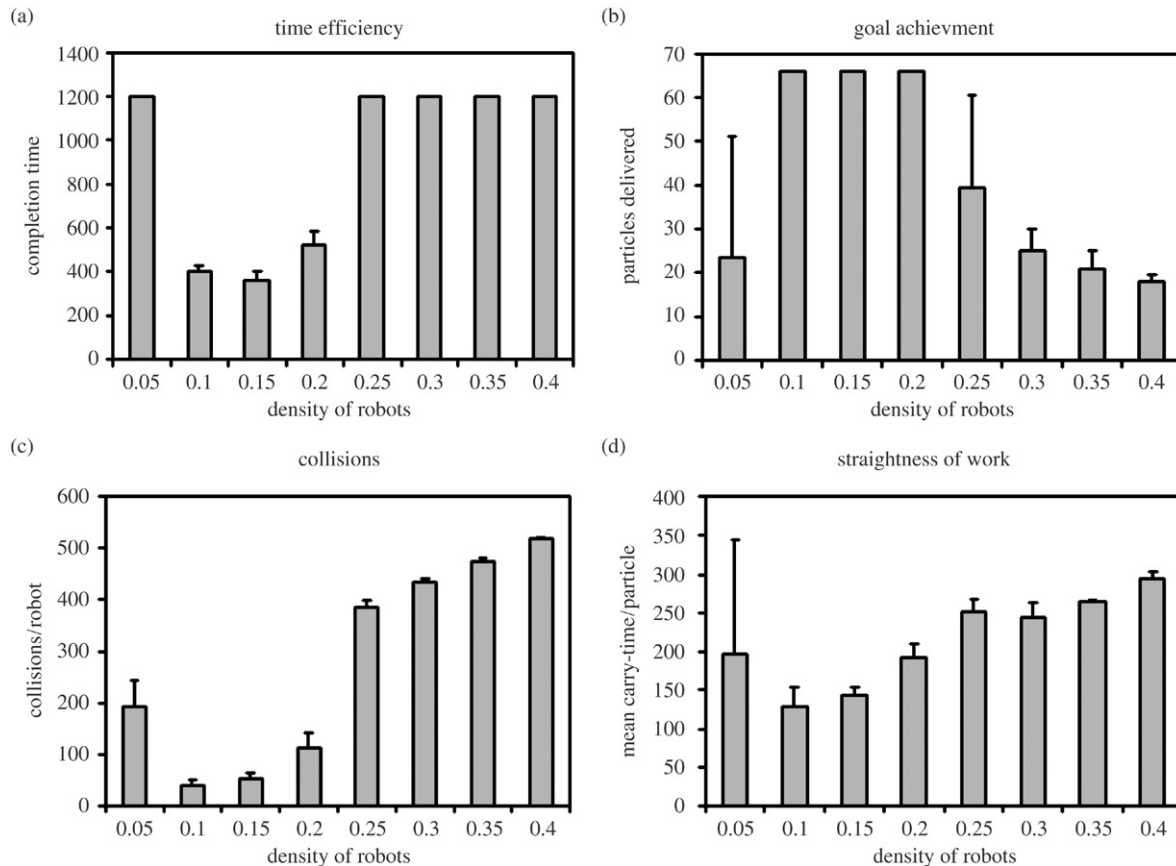


Fig. 17. The optimal density of the robot swarm is evaluated. (a) With a density between 0.1 and 0.15, the swarms finished their work in the shortest period. (b) Swarm densities between 0.1 and 0.2 allowed successful cleaning of the whole arena. (c) Swarms with densities between 0.1 and 0.15 showed the lowest collision rate per robot. (d) Densities between 0.1 and 0.15 led to the lowest mean carriage periods per dust particle. All figures show medians and third quartiles.  $N = 6$  per setting (per bar).

## Acknowledgements

The work described in this paper has been funded by the I-SWARM project (grant IST-2004-507006) of the European Community's "Future and Emerging Technologies" (IST-FET) Program. The authors wish to thank Mr. Carlo Filippeschi for his technical contribution, and Dr. Ivano Izzo for valuable discussion.

## References

- [1] H.D. Ackler, R.H. French, Y.M. Chiang, Comparison of Hamaker constants for ceramic systems with intervening vacuum or water: From force laws and physical properties, *Journal of Colloid and Interface Science* 179 (1996) 460–469.
- [2] Y. Ando, The effect of relative humidity on friction and pull-off forces measured on submicron-size asperity arrays, *Wear* 238 (2000) 12–19.
- [3] H. Aoyama, T. Santo, F. Iwata, A. Sasaki, Pursuit control of micro-robot based on magnetic footstep, in: *Proceedings of Int. Conf. on Micromech. for Information and Precision Equipment*, 1997, pp. 256–260.
- [4] D. Andel, R. Wehner, Path integration in desert ants, *Cataglyphis*: how to make a homing ant run away from home, *Proceedings of the Royal Society London B* 271 (2004) 1485–1489.
- [5] R. Beckers, O.E. Holland, J.L. Deneubourg, From local actions to global tasks: stigmergy and collective robotics, in: R. Brooks, P. Maes (Eds.), *Artificial Life IV*, MIT Press, Cambridge, 1994, pp. 181–189.
- [6] S. Beshers, J.H. Fewell, Models of division of labor in social insects, *Annual Reviews of Entomology* 46 (2001) 413–440.
- [7] E. Bonabeau, M. Dorigo, G. Theraulaz, *Swarm Intelligence: From Natural to Artificial Systems*, Oxford University Press, New York, 1999.
- [8] Y.U. Cao, A.S. Fukunaga, A.B. Kahng, Cooperative mobile robotics: antecedents and directions?, *Autonomous Robots* 4 (1997) 7–27.
- [9] N.W. Calderone, Proximate mechanisms of age polyethism in the honey bee, *Apis mellifera* L., *Apidologie* 29 (1998) 127–158.
- [10] S. Camazine, J.L. Deneubourg, N.R. Franks, J. Sneyd, G. Theraulaz, E. Bonabeau, *Self-Organization in Biological Systems*, Princeton University Press, Princeton, 2001.
- [11] G. Caprari, R. Siegwart, Design and control of the mobile microrobot Alice, in: *Proceedings of the 2nd International Symposium on Autonomous Minirobots for Research and Edutainment, AMiRE*, 2003, pp. 23–32.
- [12] B. Chang, Q. Zhou, H.N. Koivo, Experimental study of microforces in a controlled environment, in: *Proceedings of 2nd VDE World Microtechnologies Congress*, 2003, pp. 89–94.
- [13] G.S. Chirikjian, Kinematics of a metamorphic robotic system, in: *Proceedings of International Conference on Robotics and Automation, ICRA*, 1994, pp. 449–455.
- [14] M. Collett, T.S. Collett, S. Bisch, R. Wehner, Local and global vectors in desert ant navigation, *Nature* 394 (1998) 269–272.
- [15] B.V. Derjaguin, V.M. Muller, Y.P. Toporov, Effect of contact deformations on the adhesion of particles, *Journal of Colloid and Interface Science* 53 (1975) 314–326.
- [16] W. Driesen, T. Varidel, S. Régnier, J.M. Breguet, Micro manipulation by adhesion with two collaborating mobile micro robots, *Journal of Micromechanics and Micro Engineering* 15 (2005) S259–S267.
- [17] R.S. Fearing, Survey of sticking effects for micro parts handling, in: *Proceedings of IEEE/RSJ IROS*, 1995, pp. 212–217.

- [18] K.V. Frisch, Tanzsprache und Orientierung der Bienen, Springer Verlag, Berlin, 1965.
- [19] T. Fukuda, S. Nakagawa, Y. Kawauchi, M. Buss, Structure decision method for self-organizing robots based on cell structure – CEBOT, in: Proceedings of International Conference on Robotics and Automation, ICRA, 1989, pp. 695–700.
- [20] P. Gaussier, S. Zrehen, Avoiding the world model trap: An acting robot does not need to be smart, Robotics and Computer-Integrated Manufacturing 11 (1994) 279–286.
- [21] J.C. Guinot, S. Regnier, Available on line <http://micro.robot.jussieu.fr>, 2006.
- [22] K. Hosokawa, T. Tsujimori, T. Fuji, H. Kaetsu, H. Asama, Y. Kuroda, I. Endo, Self-organizing collective robots with morphogenesis, in a vertical plane, in: Proceedings of International Conference on Robotics and Automation, ICRA, 1998, pp. 2858–2863.
- [23] J. Israelachvili, Intermolecular and Surface Forces, Academic Press, London, 1985.
- [24] K.L. Johnson, K. Kendall, A.D. Roberts, Surface energy and the contact of elastic solids, Proceedings of the Royal Society of London A 324 (1971) 301–313.
- [25] T. Kazama, K. Sugawara, T. Watanabe, Collecting behaviour of interacting robots with virtual pheromone, in: Proceedings of the 7th International Symposium on Distributed Autonomous Robotic Systems, DARS, 2004, pp. 331–340.
- [26] J. Kennedy, R.C. Eberhart, Swarm Intelligence, Academic Press, San Francisco, 2001.
- [27] C.R. Kube, H. Zhang, Collective robotics: From local perception to global action, Ph.D. Thesis, University of Alberta, 1997.
- [28] J.E. Layne, W.J.P. Barnes, L.M.J. Duncan, Mechanisms of homing in the fiddler crab *Uca rapax*. 1. Spatial and temporal characteristics of a system of small-scale navigation, The Journal of Experimental Biology 206 (2003) 4413–4423.
- [29] S. Martel, M. Sherwood, C. Helm, W. Garcia de Quevedo, T. Fofonoff, R. Dyer, J. Bevilacqua, J. Kaufman, O. Roushdy, I. Hunter, Three-legged wireless miniature robots for mass-scale operations at the sub-atomic scale, in: Proceedings of the 2001 IEEE International Conference on Robotics & Automation, ICRA, 2001, pp. 3423–3428.
- [30] A. Martinoli, E. Franzi, O. Matthey, Towards a reliable set-up for bio-inspired collective experiments with real robots, in: Proceedings of the Fifth International Symposium on Experimental Robotics, ISER, 1997, pp. 597–608.
- [31] D. Maugis, Adhesion of Spheres: The JKR-DMT transition using a Dugdale model, Journal of Colloid and Interface Science 150 (1992) 243–369.
- [32] C. Melhuish, O. Holland, S. Hoddell, Collective sorting and segregation in robots with minimal sensing, in: Proceedings of the International Conference on Simulation of Adaptive Behaviour, 1998, pp. 207–216.
- [33] A. Menciassi, A. Eisnberg, I. Izzo, P. Dario, From ‘macro’ to ‘micro’ manipulation: Models and experiments, IEEE/ASME Transactions on Mechatronics 9 (2004) 311–320.
- [34] F. Mondada, G.C. Pettinaro, A. Guignard, I.W. Kwee, D. Floreano, J.L. Deneubourg, S. Nolfi, L.M. Gambardella, M. Dorigo, Swarm-Bot: A new distributed robotic concept, Autonomous Robots 17 (2004) 193–221.
- [35] S. Murata, H. Kurokawa, S. Kokaji, Self-Assembling machine, in: Proceedings of International Conference on Robotics and Automation, ICRA, 1994, pp. 441–448.
- [36] J. Ortega-Escobar, Evidence that the wolf-spider *Lycosa tarentula* (Araneae, Lycosidae) needs visual input for path integration, The Journal of Arachnology 30 (2002) 481–486.
- [37] A. Pamecha, C.J. Chiang, D. Stein, G.S. Chirikjian, Design and implementation of metamorphic robots, in: Proceedings ASME Design Engineering Technical Conference and Computers and Engineering Conference, 1996, pp. 1–10.
- [38] D. Payton, M. Daily, R. Estkowski, M. Howard, C. Lee, Pheromone robots, Autonomous Robots 11 (2001) 319–324.
- [39] L.S. Penrose, Self-reproducing machine, Scientific American 200 (1959) 105–114.
- [40] Y. Rollot, S. Regnier, J.C. Guinot, Dynamical model for the micromanipulation by adhesion: Experimental validations for determined conditions, Journal of MicroMechatronics 1 (2001) 273–297.
- [41] J.R. Riley, U. Greggers, A.D. Smith, S. Stach, D.R. Reynolds, N. Stollhoff, R. Brandt, F. Schaupp, R. Menzel, The automatic pilot of honeybees, Proceedings of the Royal Society of London B 270 (2003) 2421–2424.
- [42] S. Saito, H. Himeno, K. Takahashi, T. Onzawa, Electrostatic detachment of a micro-object from a probe by applied voltage, in: Proceedings of IEEE/RSJ IROS, vol. 2, 2002, pp. 1790–1795.
- [43] T. Schmickl, K. Crailsheim, Inner nest homeostasis in a changing environment with special emphasis on honey bee brood nursing and pollen supply, Apidologie 35 (2004) 249–263.
- [44] T. Schmickl, K. Crailsheim, Cost of environmental fluctuations and benefits of dynamic foraging decisions in honey bees, Adaptive Behavior 12 (2004) 263–277.
- [45] T. Schmickl, R. Thenius, K. Crailsheim, Simulating swarm intelligence in honey bees: Foraging in differently fluctuating environments, in: Proceedings of GECCO, 2005, pp. 273–274.
- [46] T. Schmickl, K. Crailsheim, Trophallaxis among swarm-robots: A biologically inspired strategy for swarm robotics, in: Proceedings of Biomedical Robotics and Biomechanics Conference, BioRob, 2006.
- [47] D.J.T. Sumpter, S.C. Pratt, A modeling framework for understanding social insect foraging, Behavioural Ecology and Sociobiology 53 (2003) 131–144.
- [48] K. Takahashi, H. Kajihara, M. Urago, S. Saito, Y. Mochimaru, T. Onzawa, Voltage required to detach an adhered particle by Coulomb interaction for micromanipulation, Journal of Applied Physics 90 (2001) 432–437.
- [49] R. Thenius, T. Schmickl, K. Crailsheim, The “Dance or Work” problem: Why do not all honeybees dance with maximum intensity, in: M. Pechoucek, P. Petta, L.Z. Varga (Eds.), CEEMAS 2005, in: Lecture Notes in Artificial Intelligence (LNAI), vol. 3690, Springer-Verlag, 2005, pp. 246–255.
- [50] C. Tofts, Algorithms for task allocation in ants (A Study of Temporal Polyethism: Theory), Bulletin of Mathematical Biology 55 (1993) 891–918.
- [51] U. Wilensky, NetLogo, <http://ccl.northwestern.edu/netlogo/>, 2006.
- [52] Q. Zhou, A. Aurelian, C. Del Corral, B. Chang, H.N. Koivo, Microassembly system with controlled environment, Journal of MicroMechatronics 2 (2002) 227–248.
- [53] L. Zhou, J.M. Kahn, K.S.J. Pister, Corner-cube retroreflectors based on structure-assisted assembly for free-space optical communication, Journal of Microelectromechanical Systems 12 (2003) 233–242.
- [54] Y. Zhou, B.J. Nelson, Adhesion force modeling and measurement for micromanipulation, Proceedings of SPIE, Microrobotics and Micromanipulation 3519 (1998) 169–180.
- [55] iRobots Corporation, [http://www.irobot.com/rd/p07\\_Swarm.asp](http://www.irobot.com/rd/p07_Swarm.asp), 2006.



**Pietro Valdastri** received his Laurea Degree in Electronic Engineering (with Honors) from the University of Pisa in February 2002. In the same year he joined the CRIM Lab of the Scuola Superiore Sant’Anna in Pisa as a Research Assistant. In January 2003 he started his Ph.D. in Bioengineering at CRIM Lab. His main research interests are in the field of implantable biotelemetry, MEMS-based biosensors, and swarm robotics. He is working on several European projects for the development of minimally invasive biomedical devices.



**Paolo Corradi** received his Laurea Degree in Electronic Engineering from the University of Parma in April 2002 with a thesis performed at the Microtechnology Center at Chalmers, Göteborg, Sweden. After a one-year project in optics in collaboration with the University of Parma and the Italian National Research Council, he had a job experience in the R&D department of a company working in optoelectronics. In 2004 he started his Ph.D. in Microsystem Engineering at the CRIM Lab of the Scuola Superiore

Sant'Anna, Pisa, Italy. His main research interests are in the fields of microrobotics and biomimetics.



**Arianna Menciasci** received her Laurea Degree in Physics (with Honors) from the University of Pisa in 1995. In the same year, she joined the CRIM (formerly MiTech) Lab of the Scuola Superiore Sant'Anna in Pisa as a Ph.D. student in bioengineering with a research program on the micromanipulation of mechanical and biological micro objects. In 1999, she received her Ph.D. degree by discussing a thesis titled "Microfabricated Grippers for Micromanipulation of Biological and Mechanical Objects". She had a post-doctoral position at SSSA from May 1999 until April 2000. Then, she obtained a temporary position of assistant professor in bioengineering at SSSA. Her main research interests are in the fields of biomedical microrobotics, microfabrication technologies, micromechatronics and microsystem technologies. She is working on several European projects and international projects for the development of minimally invasive instrumentation for medical applications.



**Thomas Schmickl** received his Master in Biology in 1998 and his Ph.D. in Zoology in 2001. Since then, he has been working as a Post-Doc in the laboratory "metabolism and behavior" at the Department for Zoology at the Karl-Franzens-University in Graz (Austria). His scientific topic is behavioral ecology and biological modeling. He is currently engaged in two research projects, one focusing on self-organization in honeybees and one focusing on swarms of autonomous microrobots. He teaches courses on biological modeling, including the topics self-organization, swarm intelligence and ecological models at the Department for Zoology (Graz), at the Department for Environmental System Sciences (Graz), and at the University of Applied Sciences in St. Poelten (Austria) in the course of studies "SimCom: Simulation and Computation".



**Karl Crailsheim** has a Ph.D. in Biology and Biochemistry and is a professor in the Department for Zoology at the Karl-Franzens-University in Graz as well as lecturer in the Department of Psychology. He teaches physiology, behavior and anthropology. His research is focused on insect physiology and on complex animal societies (from bees to apes).



**Joerg Seyfried** received his Master Degree in Computer Science from the University of Karlsruhe (TH) in 1996. In the same year he became research assistant at the Institute for Process Control and Robotics (IPR) of the University of Karlsruhe (TH). Since 2000 he has been the head of the group Microrobotics and Micromechatronics. In April 2003 he received his Ph.D. in engineering for work on planning and control system for microrobot-based microassembly. His main research interests are in the fields of microrobotics, planning and control of microassembly and self-organization.



**Paolo Dario** received his Dr. Eng. Degree in Mechanical Engineering from the University of Pisa, Italy, in 1977. He is currently a Professor of Biomedical Robotics at the Scuola Superiore Sant'Anna in Pisa. He has been Visiting Professor at Brown University, at the Ecole Polytechnique Federale de Lausanne, and at Waseda University. He was the founder of the ARTS (Advanced Robotics Technologies and Systems) Laboratory and is currently the Coordinator of the CRIM (Center for the Research in Microengineering) Laboratory of the Scuola Superiore Sant'Anna, where he supervises a team of about 70 researchers and Ph.D. students. He is also the Director of the Polo Sant'Anna Valdera of the Scuola Superiore Sant'Anna. His main research interests are in the fields of medical robotics, biorobotics, neuro-robotics and micro/nanoengineering. Specifically, he is active mainly in the design of miniature and microrobotics systems for endoluminal surgery, and in advanced prosthetics. He is the coordinator of many national and European projects, the editor of two books on the subject of robotics, and the author of more than 200 scientific papers (90 on ISI journals). He is Editor-in-Chief, Associate Editor and member of the Editorial Board of many international journals. He has been a plenary invited speaker in many international conferences. Prof. Dario has served as President of the IEEE Robotics and Automation Society in the years 2002–2003, and he is currently Co-Chair of the Technical Committees on Bio-robotics of the same Society. Prof. Dario is an IEEE Fellow, a Fellow of the European Society on Medical and Biological Engineering, and a recipient of many honors and awards, such as the Joseph Engelberger Award. He is also a member of the Board of the International Foundation of Robotics Research (IFRR). He is the General Chair and Program Chair of the 1st IEEE RAS/EMBS Conference on Biomedical Robotics and Biomechatronics (BioRob 2006), and the General Chair of the IEEE International Conference on Robotics and Automation (ICRA2007).